Binding of Glutamine to Glutamine-Binding Protein from *Escherichia coli* Induces Changes in Protein Structure and Increases Protein Stability

Sabato D'Auria,[1*] Andrea Scirè,[2] Antonio Varriale,[1] Viviana Scognamiglio,[1] Maria Staiano,[1] Alessio Ausili,[2] Anna Marabotti,[3] Mosè Rossi,[1] and Fabio Tanfani[2]

[1]*Institute of Protein Biochemistry, CNR, Via Pietro Castellino, 111 Naples, Italy*
[2]*Institute of Biochemistry, Faculty of Sciences, Università Politecnica delle Marche, Ancona, Italy*
[3]*Laboratory of Bioinformatics, Institute of Food Science, CNR, Avellino, Italy*

ABSTRACT **Glutamine-binding protein (GlnBP) from *Escherichia coli* is a monomeric protein localized in the periplasmic space of the bacterium. It is responsible for the first step in the active transport of L-glutamine across the cytoplasmic membrane. The protein consists of two similar globular domains linked by two peptide hinges, and X-ray crystallographic data indicate that the two domains undergo large movements upon ligand binding. Fourier transform infrared spectroscopy (FTIR) was used to analyze the structure and thermal stability of the protein in detail. The data indicate that glutamine binding induces small changes in the secondary structure of the protein and that it renders the structure more thermostable and less flexible. Detailed analyses of IR spectra show a lower thermal sensitivity of α-helices than β-sheets in the protein both in the absence and in the presence of glutamine. Generalized two-dimensional (2D) analyses of IR spectra reveal the same sequence of unfolding events in the protein in the absence and in the presence of glutamine, indicating that the amino acid does not affect the unfolding pathway of the protein. The data give new insight into the structural characteristics of GlnBP that are useful for both basic knowledge and biotechnological applications. Proteins 2005;58:80–87.** © 2004 Wiley-Liss, Inc.

Key words: glutamine-binding protein; infrared; FTIR; protein structure; 2D-IR correlation analysis; thermostability

INTRODUCTION

The *Escherichia coli* periplasmic space contains a diverse group of binding proteins whose main function is to present various molecules, such as sugars, amino acids, peptides and inorganic ions, for transport into the cell.[1] Glutamine is an important energy and nitrogen source used in the culture of eukaryotic cells.[2]

Glutamine-binding protein (GlnBP) from *E. coli* is a monomeric protein composed of 224 amino acid residues (26 kDa) responsible for the first step in the active transport of L-glutamine across the cytoplasmic membrane.[3,4] GlnBP is a member of a large family of ligand binding proteins that share the same architecture[5] and are localized in the periplasmic space of *E. coli*.[6,7] GlnBP from *E. coli* consists of two similar globular domains, the large domain (residues 1–84 and 186–224) and the small domain (residues 90–180), which are linked by two peptide hinges.[8] Each domain contains a central core of β-sheet flanked by α-helices, which is a typical β/α/β protein structure. The deep cleft formed between the two domains contains the ligand-binding site.[5] X-ray crystallographic data provide evidence that, compared to the GlnBP–glutamine complex (GlnBP–Gln), the ligand-free GlnBP exhibits a large-scale movement of the two hinges upon ligand binding, which occurs in the so-called 'flap region.'[8] Of the naturally occurring amino acids, only glutamine is bound by GlnBP, with a K_d of $3 \times 10^{-7} M$.[4]

Ligand binding proteins from the periplasmic space are also good candidates when designing highly specific biosensors for small analytes,[9] and the use of GlnBP for glutamine sensing has been explored.[10,11] When designing a protein-based biosensor or planning biotechnological applications of proteins and enzymes, detailed knowledge of structural characteristics of the macromolecules, and particularly data about protein stability, are of high importance since they are directly related to the development of the sensor.[12] In fact, practical applications of biosensors require that biomolecules be stable under a wide range of environmental conditions, as their replacement accounts for most of the operating cost. Spectroscopic techniques allow us to monitor the stability of proteins in a variety of environments and, along with X-ray analysis, are useful tools for elucidating protein structural features. In this context, and in order to obtain detailed information about the structure, thermal stability and thermal unfolding of

Abbreviations: Gln, glutamine; GlnBP, glutamine binding protein; GlnBP–Gln, glutamine binding protein in the presence of Gln; FTIR, Fourier transform infrared; Amide I′, amide I band in ^2H_2O medium; T_m, temperature of protein melting (denaturation); $T_{D1/2}$, temperature of half deuteration.

Correspondence to: Dr. Sabato D'Auria, Institute of Protein Biochemistry, CNR,Via P. Castellino 111, 80131 Naples, Italy. E-mail: s.dauria@ibp.cnr.it

Received 19 April 2004; Revised 21 June 2004; Accepted 11 July 2004

Published online 29 October 2004 in Wiley InterScience (www.interscience.wiley.com). DOI: 10.1002/prot.20289

GlnBP in the absence and in the presence of glutamine, infrared (IR) spectroscopy and computational analysis of the three-dimensional (3D) protein structure were used.

MATERIALS AND METHODS

Materials

Deuterium oxide (99.9% ^2H_2O), ^2HCl and NaO^2H were purchased from Aldrich (St. Louis, MO, USA). Tris-(hydroxymethyl)-aminomethane (Trizma base) and L-Glutamine were obtained from Sigma (St. Louis, MO, USA). All other chemicals used were commercial samples of the purest quality.

Preparation and Purification of GlnBP

GlnBP from *E. coli* was prepared and purified according to ref. 11. The protein concentration was determined using the method of Bradford[13] with bovine serum albumin as the standard on a double-beam Cary 1E spectrophotometer (Varian, Mulgrade, Victoria, Australia).

Preparation of Samples for IR Measurements

GlnBP was analyzed in 10 m*M* Tris/HCl p^{2}H 8.3, in the absence and presence of 5.0 m*M* glutamine. The p^{2}H corresponds to the pH meter reading +0.4.[14] Typically, about 2.0 mg of protein, dissolved in the buffer used for its purification, were concentrated into a volume of approximately 40 μL using a '10 K Centricon' micro concentrator (Amicon) at 3000*g* and 4°C. Afterwards, 200 μL of Tris/HCl buffer was added, and the protein solution was concentrated again. This procedure was repeated several times to completely replace the original buffer with Tris/HCl p^{2}H 8.3. Altogether, the washings took 24 h, which is the time of contact of the protein with the ^2H_2O medium prior to Fourier transform infrared (FTIR) analysis. In the last washing, the protein solution was concentrated to about 40 μL for IR measurements.

Infrared Spectra

The concentrated protein sample was placed in a thermocontrolled Graseby Specac 20500 cell (Graseby-Specac Ltd, Orpington, Kent, UK) fitted with CaF_2 windows and a 25 μm Teflon spacer. FTIR spectra were recorded by means of a Perkin–Elmer 1760-x FTIR spectrometer using a deuterated triglycine sulfate detector and a normal Beer–Norton apodization function. For at least 24 h prior to analysis, and throughout data acquisition, the spectrometer was continuously purged with dry air at a dew point of −40°C. Spectra of buffers and samples were acquired at a 2 cm^{-1} resolution under the same scanning and temperature conditions. In the thermal denaturation experiments, the temperature was raised in 5°C steps from 20 to 95°C using an external bath circulator (HAAKE F3). The actual temperature in the cell was controlled by a thermocouple placed directly onto the windows. Before spectrum acquisition, samples were maintained at the desired temperature for the time interval necessary for the stabilization of temperature inside the cell (6 min). Spectra were collected and processed using the SPECTRUM software from Perkin–Elmer. Correct subtraction of H_2O was judged to yield an approximately flat baseline at 1900–1400 cm^{-1}, and subtraction of ^2H_2O was adjusted to the removal of the ^2H_2O bending absorption close to 1220 cm^{-1}.[15] The deconvoluted parameters were set with a gamma value of 2.5 and a smoothing length of 60. Second derivative spectra were calculated over a nine-data-point range (9 cm^{-1}).

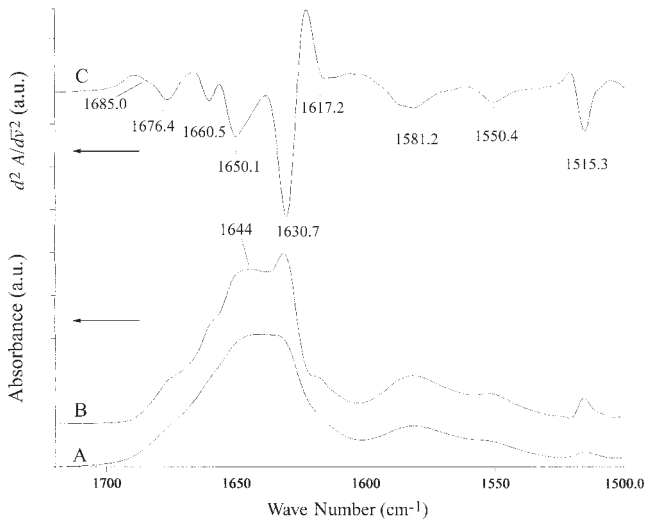

Fig. 1. Absorbance (A), deconvoluted (B), and second derivative (C) spectra of GlnBP in ^2H_2O medium at 20°C.

The temperature of protein melting (T_m) and the temperature of half deuteration ($T_{D1/2}$) were obtained by fitting the experimental data with a sigmoid function.[16]

Two-Dimensional IR Correlation Analysis

Two-dimensional (2D) correlation analysis of the IR absorbance spectra obtained at different temperatures was performed using the generalized 2D correlation procedure of Noda.[17] To generate synchronous and asynchronous spectra, 2Dcos toolbox and Matlab 6.0 software (MathWorks, Inc., Natick, MA, USA) were used. The 2Dcos toolbox was developed in Professor Ozaki's laboratory (Kwansei Gakuin University, Sansa, Japan).

RESULTS AND DISCUSSION

Structural Characterization of GlnBP and GlnBP–Gln

The absorbance and resolution-enhanced spectra of GlnBP at 20°C are shown in Figure 1. According to previous studies of proteins,[18–24] the 1650.1, 1630.7 and 1660.5 cm^{-1} bands are due to α-helices, β-sheets and turns/bends, respectively. The 1676.4 cm^{-1} peak and the small shoulder at 1685 cm^{-1} may also be due to β-sheets. However, in this case the assignment was less straightforward, since above 1670 cm^{-1} turns may also absorb.[25] The asymmetric shape of the 1650.1 cm^{-1} band in the second-derivative spectrum indicates the presence of another band at about 1644 cm^{-1} (seen in the deconvoluted spectrum) that is attributable to unordered structures. The bands below 1620 cm^{-1} are due to amino acid side chain absorption,[26,27] and the 1581.2 cm^{-1} band in particular is due to

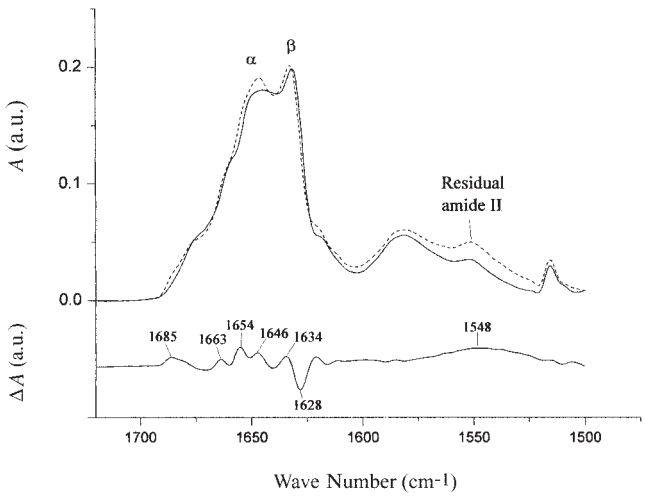

Fig. 2. Deconvoluted spectra of GlnBP in the presence and absence of glutamine in ^2H_2O medium at 20°C. Top: continuous and dashed lines refer to spectra of GlnBP in the absence and presence of glutamine, respectively. Bottom: Difference spectrum obtained by subtracting of the GlnBP spectrum from that of GlnBP–Gln (GlnBP–Gln − GlnBP).

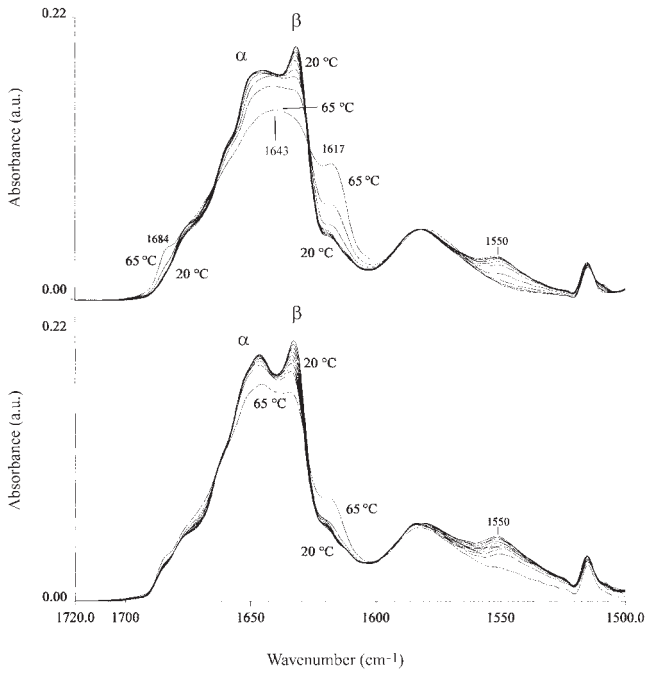

Fig. 3. Effect of temperature on deconvoluted spectra of GlnBP and GlnBP–Gln. Upper and lower panels refer to GlnBP and to GlnBP–Gln, respectively. Spectra from 20 to 65°C with 5°C increments are reported.

arginine and/or the ionized carboxyl group of aspartic acid, whereas the 1515.3 cm^{-1} peak is assigned to tyrosine.

The peak close to 1550 cm^{-1} represents the residual amide II band, i.e. the amide II band (1600–1500 cm^{-1} range) after $^1H/^2H$ exchange of the amide hydrogens of the polypeptide chain. Indeed, the amide II band is particularly sensitive to the exchange of amide hydrogen with deuterium. In experiments performed in ^1H_2O, the intensity value of the amide II band was about two-thirds that of amide I band (not shown), while in the ^2H_2O medium it decreased significantly.[28–31] The bigger the intensity decrease, the bigger the $^1H/^2H$ exchange. In turn, a big $^1H/^2H$ exchange indicates that the protein structure is very accessible to the solvent (^2H_2O). The fact that the IR spectrum of GlnBP displays a residual amide II band indicates that at 20°C the protein segments were not completely accessible to the solvent.

Figure 2 shows the superimposed spectra of GlnBP and GlnBP–Gln. The amide I′ band shapes (1700–1600 cm^{-1}) are slightly different, indicating that glutamine binding induces small changes in the secondary structure of the protein. In particular, the relative intensities of the α-helix and β-sheet bands are different, and the latter band is positioned at a higher wave number in GlnBP–Gln than in GlnBP, indicating a lower accessibility of the solvent to β-sheets.[28] This finding may be explained by the fact that, in the functional site of the protein, glutamine interacts with a number of amino acids involved in the β-sheet conformation.[5,8] As a consequence, the accessibility of the solvent (^2H_2O) to this part of the protein is reduced, and the position of the β-sheet band is shifted to higher wave numbers. The idea of reduced accessibility of the solvent to GlnBP–Gln may find further support from the higher residual amide II band intensity in the spectrum of GlnBP in the presence of the ligand. The differences between GlnBP and GlnBP–Gln spectra are better shown by the difference spectrum reported below the deconvoluted spectra. Both negative and positive peaks reflect the total changes in a particular band present in the two IR spectra to be subtracted, and their characteristics depend on a number of factors.[32] In particular, the spectrum indicates a higher intensity of the 1685 cm^{-1} band (β-sheets and/or turns) and the 1654 cm^{-1} band (α-helix) and a lower intensity of the 1628 cm^{-1} component in the GlnBP–Gln spectrum. The latter negative peak is mainly due to the shift of the β-sheets band.

Thermal Denaturation

The increase of temperature produces changes in the IR spectrum of a protein, as shown in Figure 3. The huge alteration of the amide I′ band-shape (1700–1600 cm^{-1}) is caused by a large loss of secondary structural elements that occurs markedly at temperatures above 50°C and 60°C for GlnBP and GlnBP–Gln, respectively. By increasing the temperature, the α-helix peak, and especially the β-sheet band, decrease in intensity, and at 65°C both bands disappear in the GlnBP spectrum but are still visible in the GlnBP–Gln spectrum. At 65°C, in the GlnBP spectrum, the broad band centered at about 1644 cm^{-1} is due to unordered structures. The continuous decrease in intensity of the β-sheet band, even at low temperatures, may reflect a particular thermal sensitivity of this structural element. Moreover, the spectra suggest a glutamine-dependent stability of β-sheets, as revealed by the different paths of decrease in intensity of the β-sheet band (see also Fig. 4, panel A). On the other hand, α-helices seem to be less thermo-sensitive than β-sheets (see also Fig. 4, panel B).

Figure 3 also shows two peaks, close to 1617 cm^{-1} and 1684 cm^{-1}, that start to appear at 55°C and 65°C in the

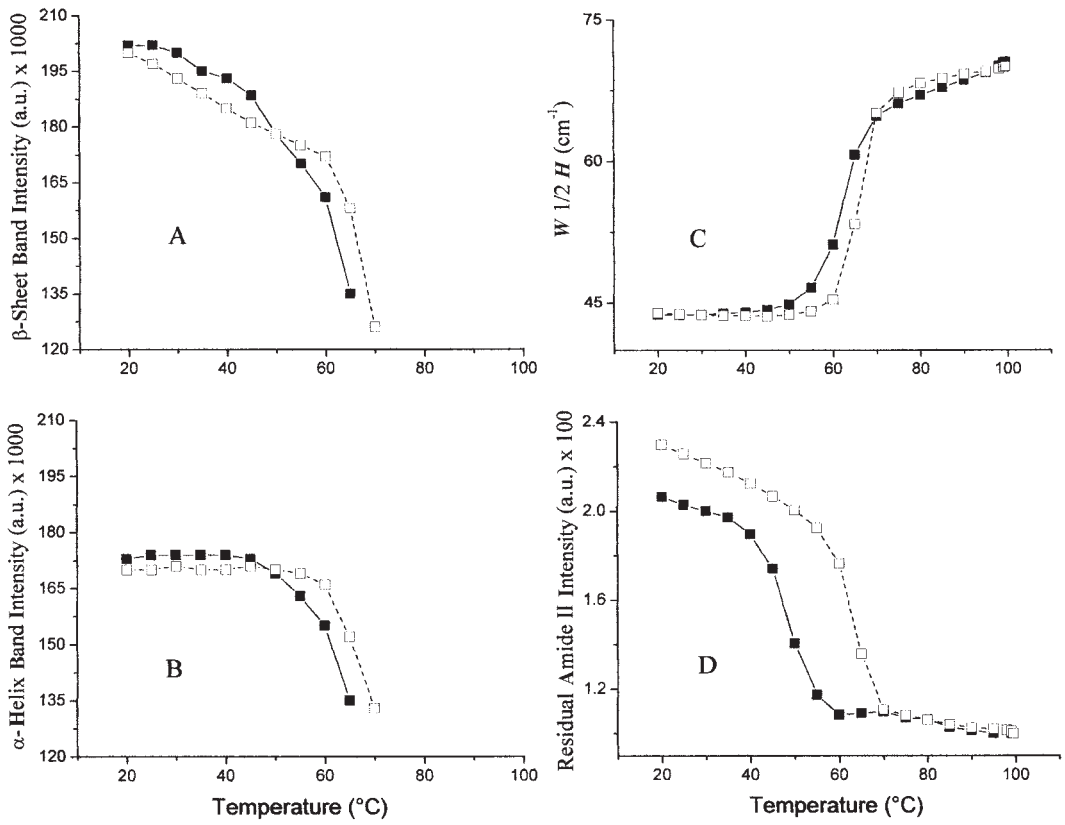

Fig. 4. Temperature-dependent changes in the characteristics of the GlnBP and GlnBP–Gln spectra. Panels (A) and (B) show the temperature-dependent changes in β-sheet and α-helix band intensity, respectively. The graphs were generated by analyzing the deconvoluted spectra. Panels (C) and (D) show the temperature-induced changes in the amide I′ bandwidth and in the residual Amide II band intensity, respectively. The graphs were generated by analyzing the absorbance spectra. (■) GlnBP; (□) GlnBP–Gln.

spectra of GlnBP and GlnBP–Gln, respectively. These two bands are due to intermolecular protein interactions (aggregation) that occur as a consequence of the denaturation process.[20,22,29] Thus, the figure shows that the presence of glutamine shifts the loss of secondary structures (denaturation) as well as the formation of aggregates to higher temperatures. Protein denaturation also induces a further $^{1}H/^{2}H$ exchange as a consequence of tertiary and secondary structure loss. As denaturation proceeds, buried amide groups become exposed to the $^{2}H_2O$ medium, and further decrease of the residual amide II band intensity at 1550 cm^{-1} occurs.

The full scenario of the above description is shown in Figure 4, which confirms that α-helices are less thermosensitive than β-sheets, both in the absence and presence of glutamine, since the intensity of the α-helix band is almost constant until 45°C in GlnBP and 55°C in GlnBP–Gln (Fig. 4, panel B), while the β-sheet band intensity decreases at 20°C (panels 4A and 4B). However, glutamine seems to exert a biphasic effect on β-sheet band intensity (panel 4A). Indeed, in GlnBP–Gln the β-sheet band intensity decreases linearly between 20 and 60°C, while in the absence of the amino acid the decrease is not linear. Moreover, the curves cross each other at about 50°C. This suggests that below this temperature glutamine could exert a destabilizing effect on β-sheets, while above 50°C the amino acid renders the secondary structural element more thermostable. Indeed, the stabilization of the structure above 50°C could be ascribed to the formation of hydrogen bonds and ionic interactions between glutamine and GlnBP. In particular, it has been noted that ion pairs could be stabilizing at high temperatures by the decrease of both the medium dielectric constant and the hydration free energies of charged residues.[33,34] It is interesting to note that the curves related to α-helix band intensity of GlnBP and GlnBP–Gln spectra (panel 4B) also cross each other at 50°C, indicating a stabilization of α-helices at high temperatures similar to that of β-sheets.

The full thermal denaturation process (panel 4C) was monitored by plotting the amide I′ bandwidth ($W\frac{1}{2}H$) as a function of temperature.[35] The width increases with the increase of the temperature as a consequence of protein denaturation and aggregation (see Fig. 3) and thus the ($W\frac{1}{2}H$) parameter monitors these two processes. The temperatures of melting (T_m) of GlnBP and GlnBP–Gln were found to be 63.1 and 66.2°C, respectively. Thus, even these curves indicate that the binding of glutamine renders GlnBP more thermostable.

Panel 4D reports the temperature-dependent decrease of the residual amide II band intensity, reflecting further $^{1}H/^{2}H$ exchange induced by the increase in temperature. In GlnBP and GlnBP–Gln, deuteration is complete at

about 60 and 70°C, respectively. The temperatures of half deuteration ($T_{D1/2}$) were found at 50.5 and 64.4°C for GlnBP and GlnBP–Gln, respectively. By comparing $T_{D1/2}$ values to T_m values, it appears that in the absence of glutamine the difference ($T_m - T_{D1/2}$) is 12.6°C, while in the presence of glutamine the difference is equal to 1.8°C. Since the extent of the $^1H/^2H$ exchange process depends on changes in the tertiary and/or secondary structure (including denaturation) of a protein, the large ($T_m - T_{D1/2}$) value in GlnBP indicates that the protein undergoes important $^1H/^2H$ exchange before denaturation, which in turn suggests that a significant relaxation of the tertiary structure precedes the loss of secondary structural elements. Indeed, if we compare panels (C) and (D), we can see that at about 50°C the further deuteration of the protein has reached its half value (panel D) while the denaturation process (panel C) has not yet begun. In the presence of the ligand, both T_m and $T_{D1/2}$ are shifted to higher temperatures, the latter to a bigger extent than T_m. Hence, the small ($T_m - T_{D1/2}$) value indicates that the relaxation of the tertiary structure is almost concomitant with denaturation (compare panels C and D), indicating in turn that glutamine induces a more compact and/or less flexible conformation[27] of GlnBP and protects the protein against temperature-induced 3D conformational changes and temperature-dependent loss of secondary structural elements.

The spectroscopic data are in good agreement with the data obtained by X-ray experiments on the crystals of GlnBP and GlnBP–Gln.[5,8] Figure 5(a) presents a view of the binding of Gln to GlnBP. The binding of the ligand causes rearrangement of the two domains of the protein in a close-cleft conformation. This allows the formation of strong interactions between the two parts of the binding site. The formation of these links increases the stability of secondary structures involved in ligand binding because they are embedded in a more rigid and compact conformation with a lower extent of fluctuation. Figure 5(b) clearly shows that the majority of the amino acids interacting with the ligand belong to β-sheets or random coils from both domains. Therefore, as a consequence of Gln binding, the formation of stabilizing interactions especially involves the β-sheets in the interior of the two domains, which are more stabilized than the α-helices. In particular, as discussed previously,[8] the binding of Gln allows the formation of a strong ionic interaction between Lys115 and Asp10, that acts as a 'door keeper' to lock Gln into the pocket cleft. As shown in Figure 5(b), both of these residues belong to β-sheets that are on opposite parts of the binding site. Thus, this interaction, along with other hydrogen bonds that are formed after closure of the binding site, may strongly lock the β-sheets into a more compact and stable conformation, probably increasing their thermal stability. On the other hand, since the contribution of α-helices to ligand binding is minor (only two residues in the binding pocket), the presence of ligand is less likely to increase the number of stabilizing interactions between these structures. Instead, a higher number of H-bonds was found for main chain–main chain interactions in α-helices compared to β-strands,[8] and this is in agreement with the higher resistance to temperature displayed by these structures in the spectroscopic measurements.

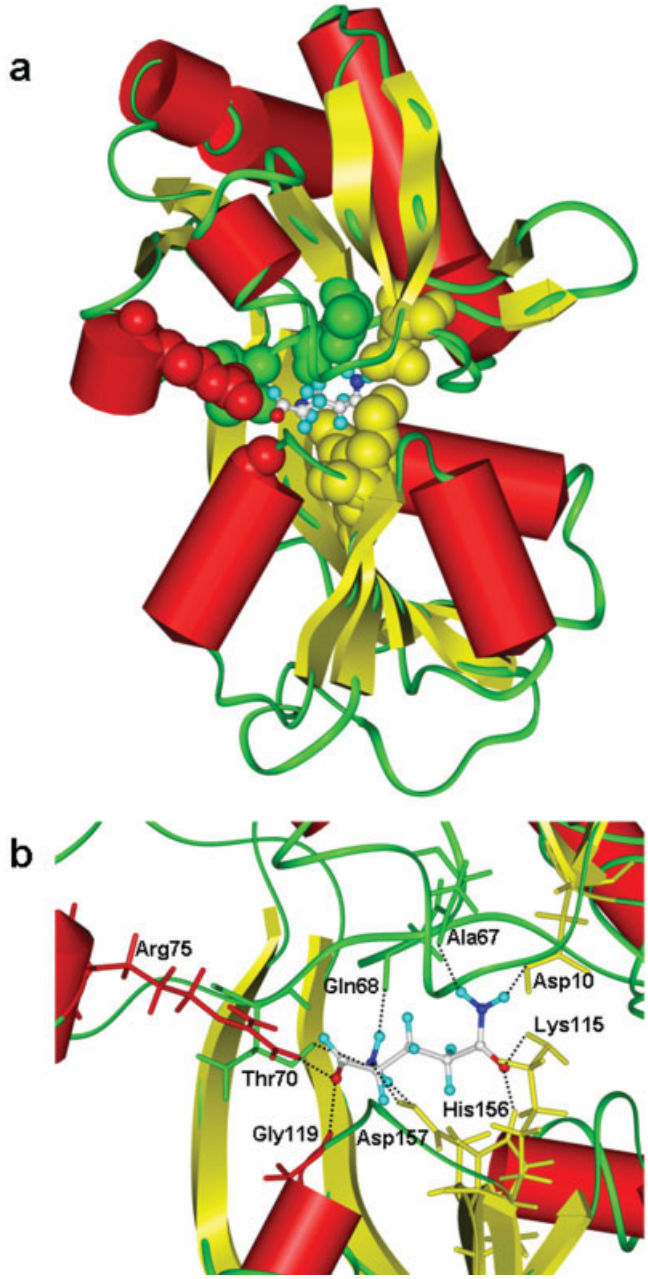

Fig. 5. Schematic view of GlnBP with Gln bound in its binding site. The picture was obtained from PDB file 1WDN.[8] Secondary structure elements are as follows: α-helices (red cylinders), β-sheets (yellow arrows) and random coil (green lines). Gln is represented in ball & stick mode and in atom type color code: white (carbon), blue (nitrogen), red (oxygen) and cyan (hydrogen). (a) Global view of the protein with the bound ligand. Residues that form H-bonds with Gln are represented in CPK mode, with colors corresponding to the secondary structures to which they belong. (b) Close-up of the binding site. Residues that form H-bonds with Gln are represented in stick mode and labeled, with colors corresponding to the secondary structures to which they belong. H-bonds are represented as dotted lines.

The fact that analysis of the crystallographic data suggests a higher stabilization of β-sheets than α-helices

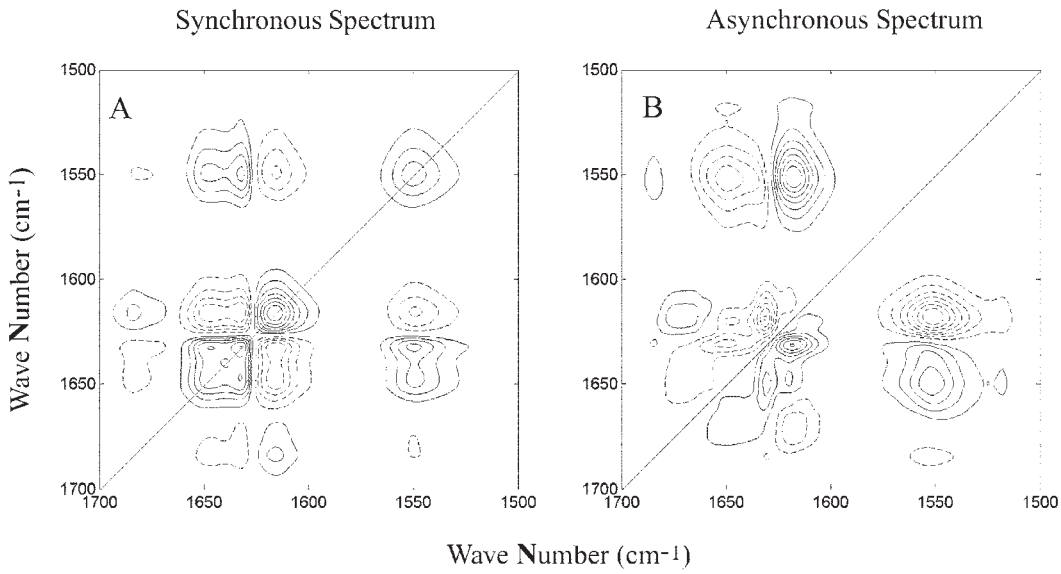

Fig. 6. Synchronous (A) and asynchronous (B) 2D-IR correlation spectra of GlnBP. Contour maps were generated using absorbance spectra collected in the 20–65°C temperature interval and the 1700–1500 cm^{-1} spectral range.

upon glutamine binding only appears to be in contrast with the IR data indicating that the binding of glutamine induces a similar thermal stabilization of the protein β-sheet and α-helix structures. In fact, it must be pointed out that the IR signal belonging to a particular secondary structure is emitted by all protein segments adopting that secondary structural motif. Hence, it may be that the structural stabilization of a particular secondary structural element is not detected because it is too small compared to the total structural characteristics of the other elements.

Thermal Unfolding Events as Monitored by Generalized 2D Correlation Analysis of IR Spectra

In order to obtain more details on the thermal stability and thermal unfolding of the protein, we applied generalized 2D correlation analysis on the infrared spectra collected at different temperatures. Generalized 2D-IR correlation analysis produces synchronous and asynchronous spectra of dynamic spectral intensity variations induced by an external perturbation (temperature, pressure, etc). The combination of asynchronous and synchronous plots provides details on the sequence of events following an applied perturbation. A synchronous spectrum represents the simultaneous or coincidental changes of spectral intensities measured at two discrete and independent wave numbers v_1 and v_2, (on x- and y-axes respectively). An asynchronous spectrum represents sequential or unsynchronized changes of spectral intensities measured at v_1 and v_2.[17] The diagonal peaks in the synchronous spectrum are referred to as autopeaks. The intensity of autopeaks represents the overall extent of dynamic fluctuation of spectral intensity observed at the specific wave number.[17] Cross-peaks in a synchronous spectrum are located in the off-diagonal position, and the signs of the synchronous cross-peaks become positive if the spectral intensities at the corresponding wave numbers are either increasing or decreasing. On the other hand, a negative cross-peak indicates that one of the spectral intensities is increasing while the other is decreasing.[17] When the system is perturbed by the increase in temperature, a positive peak in the asynchronous spectrum indicates that the spectral intensity change at v_1 occurs at a lower temperature than that at v_2. Otherwise, if the peak in the asynchronous spectrum is negative, the spectral intensity change at v_1 occurs at a higher temperature than that at v_2. This rule is reversed if the corresponding synchronous peak at v_1 (or v_2) is negative.[17] Throughout this paper, solid and dashed lines in the contour maps denote positive and negative correlation peaks, respectively.

Figure 6 shows contour maps of synchronous and asynchronous 2D-IR correlation spectra of GlnBP, generated from temperature-perturbed IR spectra. Plots were produced using absorbance spectra collected in the 20–65°C temperature interval and 1700–1500 cm^{-1} spectral range. In Figure 6(a), the main autopeaks at 1550 and 1618 cm^{-1} correspond to residual amide II and aggregation bands, respectively. The minor autopeaks at 1631 and 1650 cm^{-1} refer to β-sheet and α-helix structures bands, respectively. The appearance of the autopeaks means that the intensities of these bands vary most significantly by increasing the temperature from 20 to 65°C. The positive cross-peak at 1631^{-1} on the x-axis and 1550 cm^{-1} on the y-axis represents the correlation between β-sheets and residual amide II bands, and its sign means that the intensities of these bands are decreasing with the increase in temperature. Otherwise, the negative cross-peak at 1618 cm^{-1} and 1550 cm^{-1} indicates that the intensity of the residual amide II band is decreasing while the intensity of protein aggregation band (1618 cm^{-1}) is increasing. Table I shows the schematic representation of all peaks of the synchronous spectrum.

TABLE I. Schematic Representation of Synchronous Spectrum of GlnBP Obtained Using Absorbance Spectra from 20 to 65°C in 1700–1500 cm^{-1} Spectral Range

1550 ↓	−			+	+	−	A
1618 ↑	+	+	−	−	−	A	
1631 ↓	−	−	+	+	A		
1650 ↓	−			A			
1660 ↓							
1676 ↑							
1684 ↑							
cm^{-1}	1684 ↑	1676 ↑	1660 ↓	1650 ↓	1631 ↓	1618 ↑	1550 ↓

Peaks of the upper part of the synchronous spectrum of GlnBP (Fig. 6) are shown. Autopeaks are represented by letters (A). Positive and negative cross-peaks are represented by the signs (+) and (−), respectively, and they are described by v_1 (latter row) and v_2 (first column). The symbols (↑) and (↓) mean the increase and decrease of peak intensity, respectively.

TABLE II. Schematic Representation of Asynchronous Spectrum of GlnBP Obtained Using Absorbance Spectra from 20 to 65°C in 1700–1500 cm^{-1} Spectral Range

1550 ↓	+a			−a		+a	
1618 ↑		+b		−b	−b		
1631 ↓	+a		−a	−a			
1650 ↓		−b					
1660 ↓							
1676 ↑							
1684 ↑							
cm^{-1}	1684 ↑	1676 ↑	1660 ↓	1650 ↓	1631 ↓	1618 ↑	1550 ↓

Peaks of the upper part of the asynchronous spectrum of GlnBP (Fig. 6) are shown. They are described by v_1 (latter row) and v_2 (first column). The signs (+) and (−) represent positive and negative peaks, respectively. The letters (a) and (b) mean that the intensity change at v_1 occurs predominantly after and before v_2, respectively. The symbols (↑) and (↓) mean the increase and decrease of peak intensity, respectively.

Figure 6(b) shows the asynchronous spectrum of GlnBP. The negative cross-peak at 1650 cm^{-1} on the x-axis and 1550 cm^{-1} on the y-axis indicates that the intensity change corresponding to α-helices (1650 cm^{-1}) occurs after the change in intensity of the residual amide II band (1550 cm^{-1}). On the other hand, the positive cross-peak at 1676 cm^{-1} and 1618 cm^{-1} indicates that the intensity change of the β-sheets/turns band (1676 cm^{-1}) occurs before the change in intensity of the protein aggregation band. The full description of the asynchronous spectrum is reported in Table II. The 2D correlation analysis made on the IR spectra of GlnBP–Gln produced the same synchronous and asynchronous spectra (not shown). Since glutamine stabilizes the structure of the protein against high temperatures, the plots were generated using absorbance spectra in the 20–75°C temperature interval.

Information on the sequence of changes in intensity of the secondary structural element bands, which is the sequence of thermal unfolding events, was obtained by the analysis of both synchronous and asynchronous spectra.[17] The results indicate the following sequence: [1550 cm^{-1} ↓ ($^1H/^2H$ exchange), 1631 cm^{-1} ↓ (β-sheets), 1676 cm^{-1} ↑ (β-sheets/turns)] → [(1650 cm^{-1} ↓ (α-helices), 1660 cm^{-1} ↓ (turns/bends)]; → [(1618 cm^{-1} ↑ (protein aggregation), 1684 cm^{-1} ↑ (protein aggregation)], in which the arrows (↓ and ↑) stand for decrease and increase, respectively, of the band intensity. The events in square brackets occur concomitantly. The results indicate that the unfolding of β-sheets is the first event that occurs with the increase of the temperature and that it is accompanied by further $^1H/^2H$ exchange. The increase in intensity of the 1676 cm^{-1} band is quite surprising. However, detailed analysis of the second derivative spectra (not shown) revealed that the increase is due to a shift of the 1684 cm^{-1} band to 1676 cm^{-1}. This phenomenon is attributable to a $^1H/^2H$ exchange of β-sheets/turns, which is also consistent with the observation that the decrease of the 1550 cm^{-1} band occurs concomitantly with the shift. Unfolding of α-helices and turns/bends starts after the unfolding of β-sheets, a phenomenon that is consistent with the data shown in Figure 4(a and b). The ultimate event is the aggregation process, which is revealed by the increase in intensity of the 1618 cm^{-1} band and 1684 cm^{-1} band.

The same sequence of events was obtained for GlnBP–Gln, meaning that the stabilization of the entire protein structure against high temperatures exerted by glutamine does not change the relative stability of the secondary structural elements that undergo unfolding following the same sequence.

CONCLUSIONS

In conclusion, our data point out that the binding of glutamine to the protein induces small changes in the secondary structure of the protein, making the structure more thermostable and less flexible. In addition, a meticulous analysis of IR spectra shows a lower thermal-sensitivity of the protein α-helices than β-sheets both in the absence and presence of glutamine. The generalized

2D analysis of the IR spectra reveals the same sequence of unfolding events in the protein in the absence and presence of glutamine, indicating that glutamine does not influence the unfolding pathway of the protein.

ACKNOWLEDGMENTS

This project was realized in the frame of CRdC-ATIBB POR UE-Campania Mis 3.16 activities (S.D., M.R). This work was supported by grants from Ancona University (F.T.), F.I.R.B. (S.D., M.R.) and the Italian National Research Council (S.D, M.R).

REFERENCES

1. Higgins CF. ABC transporters: physiology, structure and mechanism: an overview. Res Microbiol 2001;152:205–210.
2. Zielke HR, Zielke CL, Azand PT. Glutamine: a major energy source for cultured mammalian cells. Fed Proc 1984;43:121–125.
3. Nohno T, Saito T, Hong J-S. Cloning and complete nucleotide sequence of the *Escherichia coli* glutamine permease operon (glnHPQ). Mol Gen Genet 1986;205:260–269.
4. Weiner JH, Heppel LA. A binding protein for glutamine and its relation to active transport in *Escherichia coli*. J Biol Chem 1971;246:6933–6941.
5. Hsiao CD, Sun YJ, Rose J, Wang BC. The crystal structure of glutamine-binding protein from *Escherichia coli*. J Mol Biol, 1996;262:225–242.
6. Higgins CF. ABC transporters: from microorganisms to man. Annu Rev Cell Biol1992;8:67–113.
7. Adams M, Oxender D. Bacterial periplasmic binding protein tertiary structures. J Biol Chem 1989;264:15739–15742.
8. Sun YJ, Rose J, Wang BC, Hsiao CD. The structure of glutamine-binding protein complexed with glutamine at 1.94 angstrom resolution: comparisons with other amino acid binding proteins. J Mol Biol 1998;278:219–229.
9. D'Auria S, Alfieri F, Staiano M, Pelella F, Scirè A, Tanfani F, Rossi M, Gryczniski Z, Lakowicz JR. Stability and structural characterization of the galactose/glucose-binding protein from *E. coli*. Biotechnol Prog 2004;6:330–337.
10. Tolosa L, Ge XD, Rao G. Reagentless optical sensing of glutamine using a dual-emitting glutamine-binding protein. Anal Biochem 2003;314:199–205.
11. Dattelbaum JD, Lakowicz JR. Optical determination of glutamine using a genetically engineered protein. Anal Biochem 2001;291:89–95.
12. D'Auria S, Lakowicz JR. Enzyme fluorescence as a sensing tool: new perspectives in biotechnology Curr Opin Biotechnol 2001;12: 99–104.
13. Bradford MM. A rapid and sensitive method for the quantization of microgram quantities of protein utilizing the principle of protein-dye binding. Anal Biochem 1976;72:248–254.
14. Salomaa P, Schaleger LL, Long FA. Solvent deuterium isotope effects on acid-base equilibria. J Am Chem Soc 1964;86:1–7.
15. Tanfani F, Galeazzi T, Curatola G, Bertoli E, Ferretti G. Reduced beta-strand content in apoprotein B-100 in smaller and denser low-density lipoprotein subclasses as probed by Fourier-transform infrared spectroscopy. Biochem J 1997;322:765–769.
16. Meersman F, Smeller L, Heremans K. Comparative Fourier transform infrared spectroscopy study of cold-, pressure-, and heat-induced unfolding and aggregation of myoglobin. Biophys J 2002;82:2635–2644.
17. Noda I. Generalized two-dimensional correlation method applicable to infrared, Raman and other types of spectroscopy. Appl Spectrosc 1993;47:1329–1336.
18. Banuelos S, Arrondo JL, Goni FM, Pifat G. Surface-core relationships in human low-density lipoprotein as studied by infrared spectroscopy. J Biol Chem 1995;270:9192–9196.
19. Byler DM, Susi H. Examination of the secondary structure of proteins by deconvolved FTIR spectra. Biopolymers 1986;25:469–487.
20. Jackson M, Mantsch HH. Beware of proteins in DMSO. Biochim Biophys Acta 1991;1078:231–235.
21. Fernandez-Ballester G, Castresana J, Arrondo JL, Ferragut JA, Gonzalez-Ros JM. Protein stability and interaction of the nicotinic acetylcholine receptor with cholinergic ligands studied by Fourier-transform infrared spectroscopy. Biochem J 1992;288:421–426.
22. Jackson M, Mantsch HH. Halogenated alcohols as solvents for proteins: FTIR spectroscopic studies. Biochem Biophys Acta 1992; 1118:139–143.
23. Arrondo JL, Muga A, Castresana J, Goni FM. Quantitative studies of the structure of proteins in solution by Fourier-transform infrared spectroscopy. Prog Biophys Mol Biol 1993;59: 23–56.
24. Muga A, Arrondo JL, Bellon T, Sancho J, Bernabeu C. Structural and functional studies on the interaction of sodium dodecyl sulfate with beta-galactosidase. Arch Biochem Biophys 1993;300:451–457.
25. Krimm S, Bandekar J. Vibrational spectroscopy and conformation of peptides, polypeptides and proteins. Adv Protein Chem 1986;38: 181–364.
26. Chirgadze YN, Fedorov OV, Trushina NP. Estimation of amino acid residue side-chain absorption in the infrared spectra of protein solutions in heavy water. Biopolymers 1975;14:679–694.
27. Barth A, Zsherp C. What vibrations tell us about proteins. Quart Rev Biophys 2002;35:369–430.
28. Osborne HB, Nabedryk-Viala E. Infrared measurements of peptide hydrogen exchange in rhodopsin. Methods Enzymol 1982;88: 676–680.
29. D'Auria S, Barone R, Rossi M, Nucci R, Barone G, Fessas D, Bertoli E, Tanfani F. Effects of temperature and SDS on the structure of beta-glycosidase from the thermophilic archaeon *Sulfolobus solfataricus*. Biochem J 1997;323:833–840.
30. D'Auria S, Rossi M, Barone G, Catanzano F, Del Vecchio P, Graziano G, Nucci R. Temperature-induced denaturation of beta-glycosidase from the archaeon *Sulfolobus solfataricus*. J Biochem 1996;120:292–300.
31. Capasso C, Abugo O, Tanfani F, Scire A, Carginale V, Scudiero R, Parisi E, D'Auria S. Stability and conformational dynamics of metallothioneins from the antarctic fish *Notothenia coriiceps* and mouse. Proteins 2002;46:259–267.
32. Umemura J, Cameron DG, Mantsch HH. A Fourier transform infrared spectroscopic study of the molecular interaction of cholesterol with 1,2-dipalmitoyl-sn-glycero-3-phosphocholine. Biochem Biophys Acta 1980;602:32–44.
33. Elcock AH, McCommon JA. Electrostatic contributions to the stability of halophilic proteins. J Mol Biol 1998;280:731–748.
34. Elcock AH. The stability of salt bridges at high temperatures: implications for hyperthermophilic proteins. J Mol Biol 1998;284: 489–502.
35. Skórko-Glonek J, Lipińska B, Krzewski K, Zolese G, Bertoli E, Tanfani F. HtrA heat shock protease interacts with phospholipid membranes and undergoes conformational changes. J Biol Chem 1997;272:8974–8982.